



Gestión del paisaje. Patrimonio, territorio y ciudad
Paisaiaren kudeaketa. Ondarea, lurraldea eta hiria
Landscape management. Heritage, territory and city

TRABAJO FIN DE MÁSTER
MASTER-AMAIERAKO LANA
FINAL MASTER'S DISSERTATION

CorTen STEEL: A SOLUTION TO ATMOSPHERIC DEGRADATION IN ACID AND MARINE ENVIRONMENTS

PATRICIA RUIZ GALENDE



2015/2016

eman ta zabal zazu



Universidad
del País Vasco

Euskal Herriko
Unibertsitatea



Gestión del paisaje. Patrimonio, territorio y ciudad
Paisaiaren kudeaketa. Ondarea, lurraldea eta hiria
Landscape management. Heritage, territory and city

Authorization of the final master's dissertation supervisor for its presentation

Dr. Kepa Castro Ortiz de Pinedo, member of the teaching staff of the master "Landscape management. Heritage, territory and city" authorizes the presentation of the work entitled:

CorTen steel: a solution to atmospheric degradation in acid and marine environments completed by Patricia Ruiz Galende under her/his supervision.

In, Leioa, 5th of July 2016

eman ta zabal zazu



Universidad del País Vasco Euskal Herriko Unibertsitatea



Gestión del paisaje. Patrimonio, territorio y ciudad
Paisaiaren kudeaketa. Ondarea, lurraldea eta hiria
Landscape management. Heritage, territory and city

Authorization of the final master's dissertation supervisor for its presentation

Dr. Julene Aramendia Gutierrez, member of the teaching staff of the master "Landscape management. Heritage, territory and city" authorizes the presentation of the work entitled:

CorTen steel: a solution to atmospheric degradation in acid and marine environments completed by Patricia Ruiz Galende under her/his supervision.

In, Leioa, 5th of July 2016

eman ta zabal zazu



Universidad del País Vasco Euskal Herriko Unibertsitatea

INDEX

1. INTRODUCTION	1
1.1. WEATHERING STEEL	1
1.1.1. Protective layer formation	2
1.1.2. Structure of protective layer	3
1.2. DETERIORATION AND DECAYING MECHANISMS	3
1.2.1. Sulphur dioxide	4
1.2.2. Nitrogen compounds	4
1.2.3. Chloride in marine environments	5
1.3. POSSIBLE SOLUTION: ION EXCHANGE RESINS	6
2. OBJECTIVES	8
3. EXPERIMENTAL PROCEDURE	9
3.1. DESCRIPTION OF THE SAMPLES	9
3.2. MATERIALS AND METHODS	11
3.2.1. Potentiometry	11
3.2.2. Raman spectroscopy	12
3.2.3. Infrared spectroscopy	13
3.2.4. Handheld Electron Dispersive X-Ray Fluorescence Spectroscopy (EDXRF) ...	13
3.2.5. Ion exchange resin treatment	14
3.2.6. Determination of soluble salts	14
3.2.7. Inductively Coupled Plasma – Mass Spectrometry (ICP-MS)	16
3.2.8. Chemical and thermodynamic modelling	16
4. RESULTS AND DISCUSSION	17
5. CONCLUSIONS	29
6. BIBLIOGRAPHY	32
7. APPENDIX	36
7.1. SCIENTIFIC PUBLICATIONS	36
7.1.1. Articles	36
7.1.2. Congresses	36

1. INTRODUCTION

Nowadays, steel is one of the most common materials widely used in the modern society for structural and functional applications. Actually, steel has been the main material for different sectors since the beginning of Iron Age, playing still today very important roles in the world ¹.

Steels are iron base alloys which contain carbon, generally in less content than 2%, and other alloy elements. They are classified on the basis of composition. On the one hand, the so called unalloyed steels can be found, which are divided in different groups depending on its carbon content. On the other hand, there are alloyed steels, made by mixing iron and carbon with small amounts of several alloy elements which give to the steel an improvement in its properties ².

Inside this last group, the so called *weathering steels* can be found. These are high-strength low alloy steels whose alloy elements help to develop a special atmospheric corrosion resistance due to the formation of a self-protection layer ^{3, 4}. The amount of alloying elements, which commonly are Cr, Cu, Si and P among others, varies between 1 and 2.5%. The presence of these alloy elements promotes the development of a protective rust layer. The formation of this rust layer depends on the access of oxygen in presence of moisture and air. After several wet/dry cycles, this layer system developed with time, becomes protective by preventing further access of oxygen and moisture, and therefore, reducing considerably the corrosion rate ³.

Due to this fact, this material has been also widely used with artistic aims. Its colour and texture become crucial for artists. These rust characteristics depend upon the nature of the environment and exposure time. For instance, in an industrial atmosphere, the weathering process generally is more rapid and the final colour becomes darker. In contrast, on rural environments, the oxide formation is usually slower and the colour gets lighter ⁵. It is for this capability of controlling hues and appearance that this kind of steel is widely used in outdoor structures and it is in vogue among modern artists, being some of these structures considered as Cultural Heritage.

1.1. WEATHERING STEEL

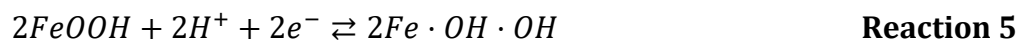
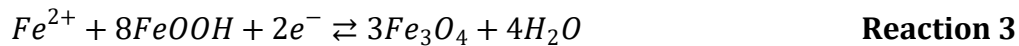
As it has been mentioned above, this type of steel develops a characteristic rust layer that protects the metal by reducing the corrosion rate. This process is known as self-protection and it is favoured by the presence, among other factors, of alloy elements,

where each one plays its own role ⁶. In this work, CorTen steel, which is the best-known commercial trademark and one kind of weathering steel, was analysed.

1.1.1. Protective layer formation

The corrosion process of weathering steel and the reactions that lead to the formation of the rust layer are the same as those of regular steels. In fact, the only difference is the effect of the alloy elements, which help on the formation of the protective rust layer on weathering steels, which is formed by reaction of iron and those alloy elements with reactive species such as water and SO₂. To better understand this corrosion process it is necessary to know what a wet/dry cycle is and how it affects to the development of the protective rust layer ^{7,8} since these cycles are crucial on the correct formation of a well packed rust layer.

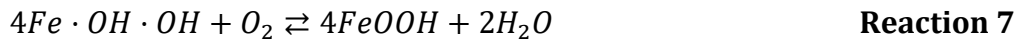
Atmospheric corrosion of iron is an electrochemical process and it can be divided into three stages (related with wet/dry cycles): the first one, the wetting of the dry surface, the second one, which is the wet surface, and finally, the drying-out of the surface. The first one occurs when the anodic reaction (Reaction 1) takes place, and part of the metallic iron is dissolved into ferrous ions. The rusting of steel in the atmosphere is given by Reaction 2 where the oxygen oxidizes other part of metallic iron to Fe³⁺, which in contact with water forms the corresponding oxyhydroxide. The two electrons generated in Reaction 1 will be used in cathodic partial reduction of the oxyhydroxide to magnetite (Reaction 3). The magnetite will be re-converted into FeOOH (Reaction 4) thanks to the atmospheric oxygen. The resulted FeOOH can be reduced also following the Reaction 5.



During the first step, after all reducible FeOOH is consumed, the oxygen reduction starts becoming the cathodic reaction (Reaction 6).



Finally, in the drying stage, the oxygen is able to re-oxidize the Fe^{2+} previously formed (Reaction 7).



All wet/dry process is represented in Figure 1.1. The formation of the protective layer requires these cycles to be well formed, the wetting to generate the rust and the drying to allow it to recrystallize^{3, 5, 9}.

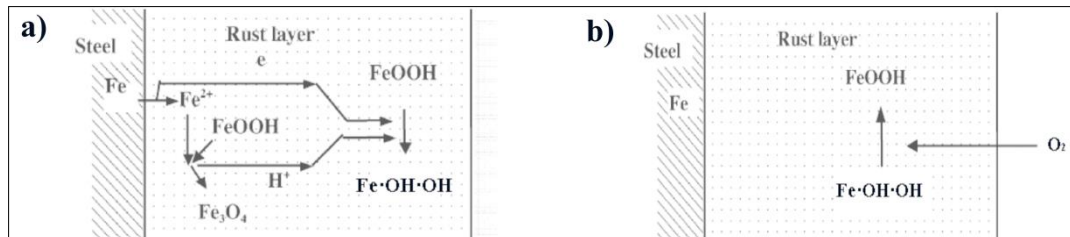


Fig 1.1. Rust layer formation. a) Wet conditions, the reduction of FeOOH of the rust and oxidation of substrate steel take place. b) Dry conditions, the rust layer partially reduced is re-oxidized by O_2 .

1.1.2. Structure of protective layer

The first compound formed at early stages of rusting is lepidocrocite ($\gamma\text{-FeOOH}$) and part of it is transformed into goethite ($\alpha\text{-FeOOH}$) with the exposure time. This process is promoted by alloying elements, which enable the formation of an uniform layer of the corrosion product by promoting the formation of $\gamma\text{-FeOOH}$. Misawa et al.¹⁰ investigated first the mechanism of formation of rust layer in aqueous solution and identified amorphous oxyhydroxide ($\text{FeO}_x(\text{OH})_{3-2x}$), together with $\alpha\text{-FeOOH}$ and $\gamma\text{-FeOOH}$. Under dry and oxidising conditions, when oxygen is able to enter into the rust layer, the magnetite (Fe_3O_4) is oxidised to amorphous FeOOH, which is again transformed into crystalline α or $\gamma\text{-FeOOH}$. Most of the authors have indicated that long-term exposure experiments are a key point in terms of protective rust formation on weathering steels. Moreover, they also supported the fact that the early stages of the exposure determine the subsequent corrosion rate^{5, 8}.

1.2. DETERIORATION AND DECAYING MECHANISMS

The ability of weathering steels to fully develop their anticorrosive action is dependent on the exposure conditions of the metallic surface. For the proper development of the rust layer, acid gases are necessary. However, when the quantity of these acid gases is too high, the soluble salts formed can increase the corrosion process, being sulphur dioxide the most studied contaminant. Besides, the increasing presence of other gases, like NO_x , has fostered the study of their effects. Furthermore, other compounds such as

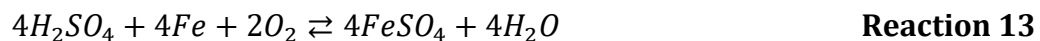
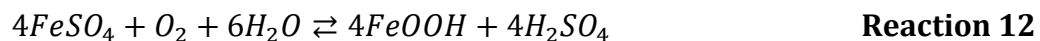
chloride can influence seriously the formation of rust layer, especially in coastal environments ^{11, 12}. The high amount of acid gases and a high humidity can cause aesthetical problems on the structures, which could lead into structural damages, such as holes, detachments of steel chips, discolorations and irregularities due to the increase of the corrosion rate of the steel. Sometimes this type of problems forces the removal of sculptures or their demolition ¹³.

1.2.1. Sulphur dioxide

Sulphur dioxide (SO₂) is dissolved in water and high concentrations of it decrease the pH enhancing the corrosion rate of the steel as following reactions show:



Part of the dissolved SO₂ may be oxidized to SO₃ producing H₂SO₄, while another part is absorbed on the metal surface reacting with iron to produce FeSO₄ (Reaction 11). This soluble salt reacts with the atmospheric oxygen generating iron oxyhydroxide and sulphuric acid (Reaction 12) which attack the surface regenerating the soluble sulphate (Reaction 13) ⁹.



The presence of soluble salts of iron promotes the leaching of iron cations to the soil and to the ground waters.

1.2.2. Nitrogen compounds

Nitrogen oxides are the major components in the troposphere. The most frequently nitrogen oxide is nitric oxide (NO), which oxidizes to nitrogen dioxide NO₂, which are the precursors of nitrous and nitric acids. Due to their slow reaction kinetics and low water-solubilities can acidify the water film formed on metal surfaces (Reaction 14). This acidification can happen in presence (Reaction 15) and absence (Reaction 16) of oxygen. These reactions can be followed by a thermal decomposition of nitrous acid into nitric oxide and nitric acid ¹⁴.



As happens in the case of the sulfuric acid, nitric acid reacts with the iron forming the corresponding nitrates, which are very soluble. These soluble nitrates are another origin of iron cations leaching.

Besides, NO₂ and SO₂ have a synergistic effect, which is based on the fact that the presence of nitrogen oxides enhances the subsequent absorption of sulfur dioxide ¹⁵.

1.2.3. Chloride in marine environments

Chloride ion is one of the most important natural particulate materials in atmospheric environments. In presence of a higher chloride concentration, there is a harmful effect on the corrosion kinetics, rust composition and structures, i.e. accelerating the rate of corrosion through the modification of redox potentials of iron. Akaganeite (β -FeOOH) is typical of coastal environments. It is formed in the surface of steel in high amount of Cl-containing environment, and can work as a reservoir of chloride ions in the metal. In addition, the presence of this compound in the rust layer increases its porosity and facilitates the transmission of chloride and other stressors from outside, which finally accelerates the corrosion process ^{3, 16}. Nomura et al. ¹⁷, noted that lepidocrocite was formed on the surface of the rust surface where the oxygen is available, whereas the formation of akaganeite takes place in the inner part of the rust layer, at the steel/rust interface, where the access of oxygen from the air is more limited but where the damage is higher.

Besides, not only iron can leach, but also other metals such as manganese or nickel can leach in sulphate or nitrate form ³. Taking all this into account, it is necessary to study the behaviour of weathering steel under urban polluted atmospheres and marine environments in order to preserve the Cultural Heritage elements made of this alloy. In this way, the destruction of the sculptures due to the increase of corrosion rate could be avoided, and several negative environmental impacts due to the toxicity of the metals that compose the steel and which are leached as soluble salts could be prevented.

In order to prevent metal leaching, because of the problem caused by anionic compounds, in this research work it was proposed the use of ion exchange resins.

1.3. POSSIBLE SOLUTION: ION EXCHANGE RESINS

Nowadays, resins are likely the most widely used material for ion exchange and they have some advantages such as uniform quality, several types to choose from, hydraulic properties and the ability to be manipulated to increase efficiency. These are the reasons why, ion exchange based resins had been proposed as a method for removal of the previously described soluble salts and chlorides ¹⁸.

Synthetic ion exchange resins (Fig 1.2) are based on polymers which are able to exchange ions between the polymer and other ions in solutions or surfaces that are in contact with them. They are cross-linked polyelectrolytes with an uniform distribution of ionic functional groups attached by covalent bond to the polymeric matrix. Exchange materials are spheres with specific size and uniformity to fulfil the needs of a specific application. To preserve electro neutrality, a same number of ions and counter ions, have to be present ¹⁹. The exchanges occur without any alteration into the resin, allowing the regeneration of that resin. Therefore, when the resin is saturated, after a simple post-treatment, it will be ready for another exchange operation reducing the possible environmental impact that would involve its management or elimination. These synthetic exchangers are generally divided into four groups depending on the resin functional group, which determines whether cations or anions are exchanged and whether the resin is a strong or a weak electrolyte (Table 1.1). If the resin is in cation form, it has exchangeable positive ions in a negatively charged matrix. However, if the resin is in anion form, matrix is positively charged and the exchangeable ions are negative ^{20, 21}.

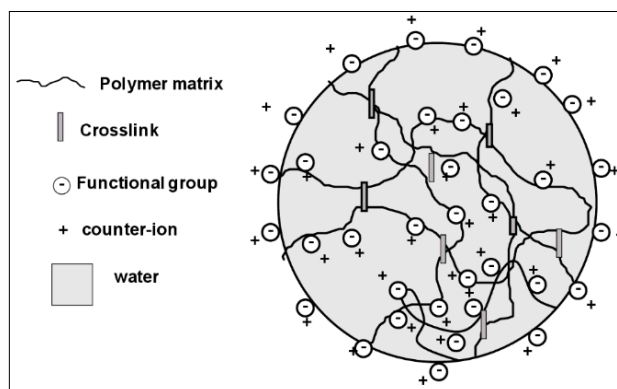
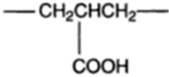
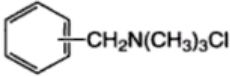
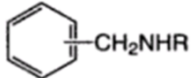
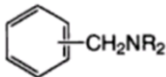


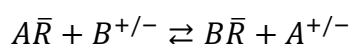
Fig 1.2. Schematic representation of a cation exchanger resin

Table 1.1. Classification of ion exchange resins

TYPE	ACTIVE GROUP	TYPICAL CONFIGURATION
Cation Exchange Resins		
Strong acid	Sulfonic acid	

Weak acid	Carboxylic acid	
Anion Exchange Resins		
Strong Base	Quaternary ammonium	
Weak base	Secondary amine	
Weak base	Tertiary amine (aromatic matrix)	

The exchange will take place (as following Reaction 17) when a resin (R) with an ion A, has a better affinity for ion B, which is in the material the resin is in contact with. The exchanger R in A form is able to exchange for B replacing it with an equivalent quantity ²¹.



Reaction 17

All these resins have some chemical properties in common that are important when they are used:

Capacity. It refers to total number of sites available for exchange. It is expressed on a dry weight, wet weight or wet volume. Capacity depends on the nature of the polymer and on the environment in which the sample is placed ²¹.

Swelling. It is related to the hydration of the fixed ionic groups. Resin volumes change with conversion to ionic forms with different degrees of hydration ²¹.

Kinetics. It means the speed that exchange happens with. Uniform particle sized resins show increased kinetic performance ²¹.

Stability. It depends on the resin type or the ion that it is wanted to change. Stability also is dependent on temperature and pH ²¹.

2. OBJECTIVES

The main objective of this final master's dissertation was to evaluate the damage caused in weathering steel structures due to the effect of different environmental stressors. These stressors are compounds like acid gases (SO_2 or NO_x) and chlorides which, moreover, it has been demonstrated that they have a key role in this material deterioration process and in material loosing³.

To accomplish that objective, different experiments were carried out.

On the one hand, accelerated corrosion tests will be performed in order to see the redox potential trend and the kinetic of the metal leaching. In this way, it will be possible to relate the potential trend with the protective layer formation. Besides, determining the composition of the sample surface is another purpose to assure the presence of soluble salts which are the responsible of the structural damage. In addition, the effect that the leaching of metals in a porous material, such as a calcite ground, could cause will be evaluated in order to compare this situation with a real one. In this way, the stained caused on the ground where weathering steel structures are placed will be better understand. Moreover, the importance of the environment in which the structures are exhibited will be checked.

On the other hand, a sample exposed to the weather will be analysed due to the similarities with a real situation, in order to check a solution for the structural damage described in the Introduction by employing ion exchange resins. The aim is to remove the described compounds that are increasing the corrosion rate of the steel.

3. EXPERIMENTAL PROCEDURE

3.1. DESCRIPTION OF THE SAMPLES

The weathering steel pieces analysed were obtained from the casting that was used for a sculpture (*Besarkada XI*) made by the Spanish sculptor Eduardo Chillida (Fig 3.1). This sculpture is exhibited outdoors in Bilbao city (Northern Spain), which is subjected to a corrosive atmosphere because of the high humidity and the presence of acid gases³. Due to this fact, it is suffering a detaching process that makes the surface heterogeneous and due to this fact the access of harmful compounds becomes easier. The steel used for the artwork is a special type of CorTen A steel that has an amount of copper lower than conventional CorTen A.

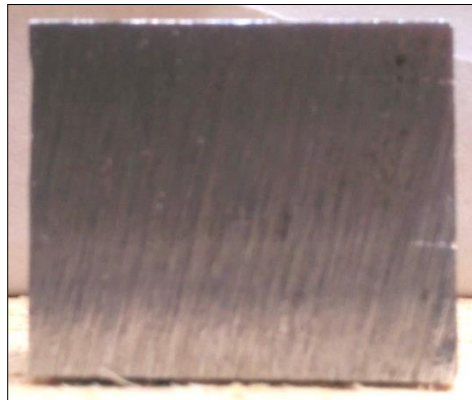


Fig 3.1. CorTen steel pieces without protective layer

The composition of the material is summarized in Table 3.1. Therefore, the attainment of this study will help in the comprehension of the conservation problems (described in the Introduction section) of the mentioned sculpture without the necessity of performing any sampling procedure.

Tabla 3.1. Composition (%) of Besarkada XI's CorTen steel

C	S	P	Si	Mn	Ni	Cu	Cr
≤0,07	≤0,02	0,08-0,13	0,25-0,4	0,3-0,5	0,3-0,6	0,15-0,35	0,75-1

Due to the problems that this type of material can suffer in polluted or marine environments a simulation of outdoor conditions was done. For that purpose, an accelerated aging experiment was carried out immersing steel pieces (2,4x2cm; ~20g) (Fig 3.2. a)) in synthetic rainwater during, at least, two weeks. This rainwater was prepared with the following inorganic salts dissolved in 1 liter of deionized water²²:

NaNO_3 (4.07 g); NaCl (3.24 g); KCl (0.35 g); $\text{CaCl}_2 \cdot 2\text{H}_2\text{O}$ (1.65 g); $\text{MgSO}_4 \cdot 7\text{H}_2\text{O}$ (2.98 g); and $(\text{NH}_4)_2\text{SO}_4$ (3.41 g). The resulting solution had a pH of 5.3.

Besides, a piece ($7 \times 5 \text{ cm}^2$; $\sim 130 \text{ g}$) exposed to the weather during 4 years (Fig 3.2. b)), was analysed. This sample was placed in a balcony near to a high transited road and an estuary. Therefore, it was affected by polluted gases and marine airborne. With this sample, it was pretended to check the damage of a sample in a real environment and with an exposition time halfway between a short-term and long-term exposure experiments.

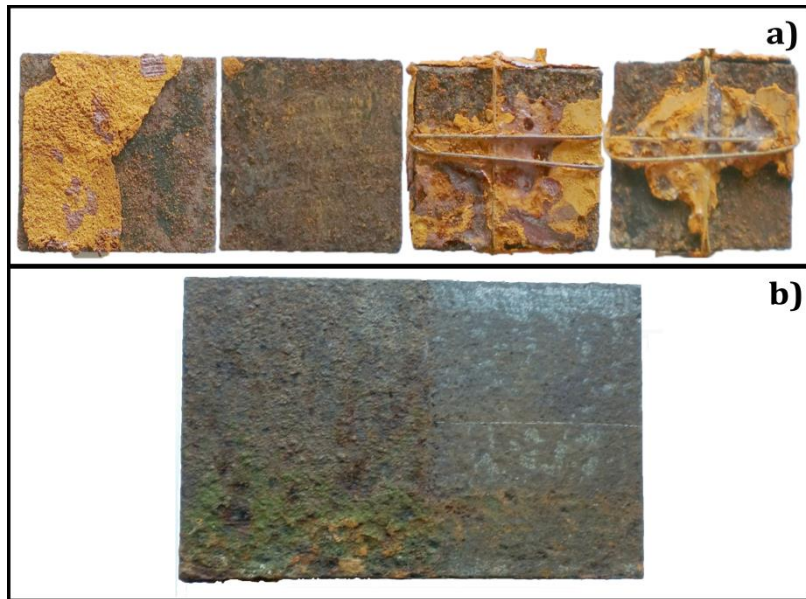


Fig 3.2. a) Pieces immersed in synthetic rainwater; b) Piece exposed outdoors

On the other hand, another steel sample was placed over a marble slab (Fig 3.3), and was sprayed with the prepared acid rain daily for two months. The marble slab had an inclination angle of 45° in order to study the run-off of the metal and the stained effect of the iron, and other metals, over the porous material.

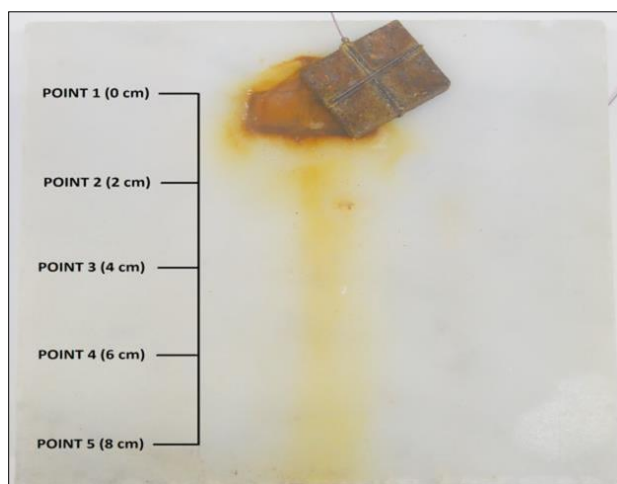


Fig 3.3. Analysed marble slab indicating the points where EDXRF analyses were done

3.2. MATERIALS AND METHODS

3.2.1. Potentiometry

In order to see the redox potential trend of the solution in which the samples subjected to the accelerated aging were immersed, potentiometric measurements were carried out. For that purpose a platinum electrode (Metrohm Ion Analysis) and Ag/AgCl reference electrode (Crison) were immersed together with the samples under magnetic stirring and inside a thermostatic bath (25°C, Fig 3.4). Home-made software called POTTIE ²³ was used to acquire the redox potential during the experiments. As it has mentioned before, these experiments had a duration of at least, two weeks, taking data every 864 seconds.

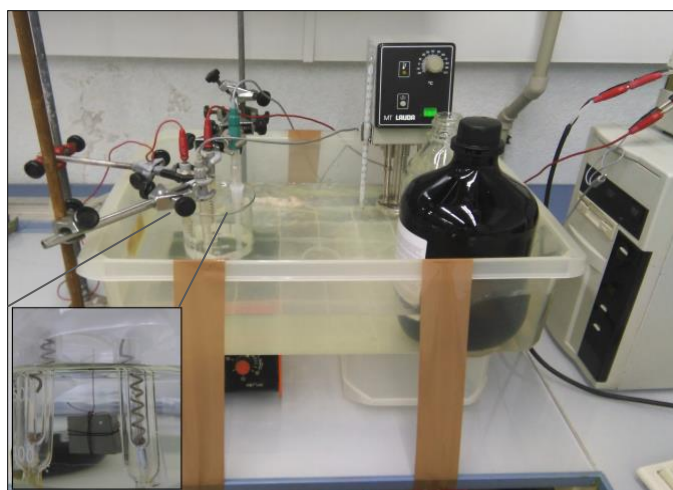


Fig 3.4. Thermostatic bath of potentiometric experiment

3.2.2. Raman spectroscopy

By means of this technique the samples were analysed to characterise the protective layer and the degradation products formed in the steel surface. The samples were analysed directly without any preparation step. On the one hand, a hand-held InnoRam spectrometer by BWTEC_{INC} (Fig 3.5. a)) was used with a 785 nm excitation laser, 20x long range objective and with a Charge Couple Device (CCD) detector (Peltier cooled). The spectroscopic data were acquired with the BWSpec™ software version 3.26. On the other hand, a Renishaw inVia Raman micro spectrometer (Fig 3.5. b)), provided with a 532 nm laser as excitation source, with 20x objective and a CCD detector was used. In this case, the software used for the data collection was the Wire 4.2 and the equipment was installed on antivibratory table.

In all cases, laser powers lower than 20mW were used to avoid the thermodecomposition of the samples and mineral phases changes. Acquisition times as well as the number of scans were set to optimum values in order to obtain a good signal to noise ratio. The calibration of the instruments was performed every day by using a silicon slice with the 520,5 cm⁻¹ band.

For spectral analysis and treatment, the Omnic software by Thermo Nicolet was used. The spectra interpretation was performed by comparison with standard spectra contained in home-made spectral database ²⁴, with the RRUFF™ on-line database and bibliography ^{3, 25, 26, 27, 28, 29}. In addition, when broad bands appeared, deconvolutions were performed with GRAMS32 (Thermo Scientific) software based on Lorentzian and Gaussian functions.

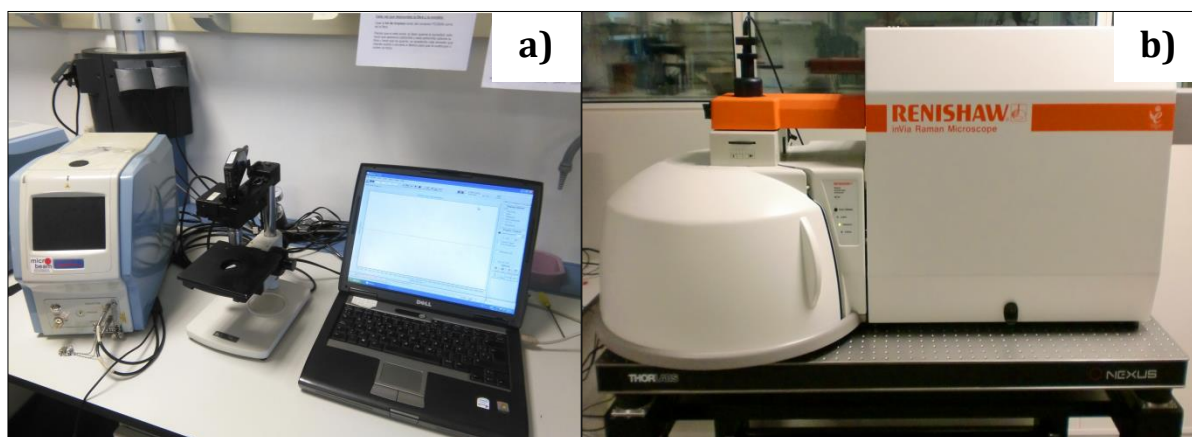


Fig 3.5. a) InnoRam BWTECINC Raman spectrometer. b) Renishaw InVia Raman micro spectrometer

3.2.3. Infrared spectroscopy

Through this technique the pieces immersed in acid rain were analysed in order to support the results obtained by Raman spectroscopy because some compounds were very difficult to identify by means of the last technique. The infrared spectra were acquired with a Jasco 6300 FT/IR spectrometer (Fig 3.6). The system has a Ge/KBr beam splitter and DLATGS detector with Peltier temperature control. All spectra over the 400-4000 cm^{-1} range were obtained by the co-addition of 64 scans with a resolution of 4 cm^{-1} . In this regard, it was necessary the preparation of pellets because the measurements were performed in transmittance mode. For that purpose, 0,5 mg of sample (the oxide layer formed in the steel surface scratched using a scalpel) were mixed with 200 mg of KBr in an agate mortar, transferred to a metallic die, and then a total pressure of 8 tons was applied. For the spectra acquisition Spectra Manager (JASCO) software was used and for the spectral analysis and treatment Omnic software was employed. The interpretation of the bands was performed by comparison with bibliography^{30, 31, 32}.



Fig 3.6. Jasco 6300 FT/IR spectrometer

3.2.4. Handheld Electron Dispersive X-Ray Fluorescence Spectroscopy (EDXRF)

In order to determine the elemental composition of the samples a hand-held Electron Dispersive X-Ray Fluorescence (EDXRF) portable analyzer XMET5100 (OXFORD Instruments) was used (Fig 3.7). The equipment is provided with a rhodium X-Ray tube as excitation source that works at a maximum voltage of 45 kV and includes a high resolution silicon DRIFT detector (SDD). Before the analysis of samples, a reference steel material was analyzed to check the EDXRF system and to select the most appropriate method. The software by Oxford implements a so called Alloy LE method that provides accurate quantitative data for metallic alloys. The used experimental conditions were 70 seconds and 5 replicates.



Fig 3.7. Handheld EDXRF portable analyser XMET5100 (OXFORD Instruments)

3.2.5. Ion exchange resin treatment

The resin treatment was performed by employing an ion exchange resin, Purolite A-100. It is a macroporous polystyrenic weak base anion resin having tertiary amine functionality. It is designed to exhibit high capacity in removing strong acids such as Cl^- , NO_3^- and SO_4^{2-} ³³.

As the resin is in Cl^- form it was necessary to prepare the resin keeping it under water for at least 40 h ³⁴ to change the chloride ions for hydroxide ions. Then, for the piece treatment, 15 g of resin were mixed with 0,15 g of methyl-cellulose and this mixture was applied in the sample during 48 h ³⁵ (Fig 3.8).

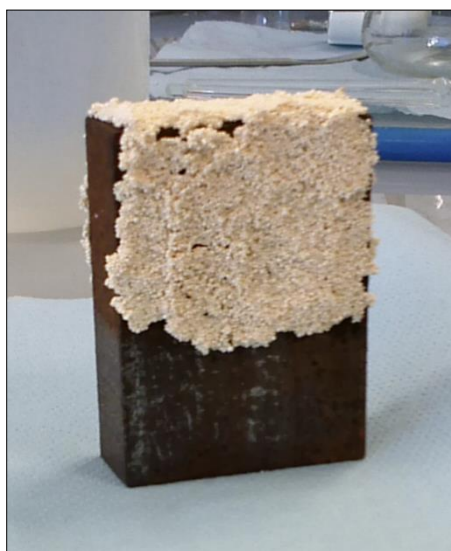


Fig 3.8. Resin applied on the steel sample

3.2.6. Determination of soluble salts

By means of Ion Chromatography (IC) the sample exposed to the weather during 4 years was analyzed. As it has been mentioned in the Introduction section, with the resin treatment it was pretended to remove some anions, exactly those which affect more to

the Corten Steel ³. Hence, it was necessary to quantify the salts present in the steel before and after that treatment in order to evaluate its effectiveness. Besides, this sample is very similar to the real sculpture (*Besarkada XI*) since they are made of the same material and exposed to comparable atmospheres. This fact allowed avoiding performing the essays over the real artwork since it was unknown if the resin treatment could change its colour or texture.

To perform this, the pre-treatment of the samples was required. The samples were obtained from the surface of the piece with the help of a scalpel and then they were grinded using an agate mortar. The protocol followed is an adaptation of one proposed by the Society of Protective Coatings (SSPC) ³⁶. The treatment carried out consists on introducing 0,1 mg of sample in 5 mL of deionized water, heating until the boiling point. The sample must be boiling for 45 minutes. Along this time, if liquid evaporated it had to be replenished up to 5 ml. After the extraction time, the extract was filtered with a 0,45 μm Millipore filter and preserved at 4°C.

The quantification of the anions and cations of the soluble salts present in the steel surface was carried out using a Dionex ICS 2500 ionic chromatograph with a suppressed conductivity detector ED50 (Fig 3.9). An IonPac AS23 (4x250 mm) column and IonPac AG23 (4x50 mm) pre-column were used for separation of anions (chloride, sulphate and nitrate). The quantification of cations (sodium, calcium, potassium and ammonium) was conducted by using an IonPac CS12A (4x250 mm) column and IonPac CG-12A (4x50 mm) pre-column by Vertex. 5 mM Na_2CO_3 /0.8 mM NaHCO_3 buffer and 25 mA suppression current at 1 $\text{mL}\cdot\text{min}^{-1}$ flow were set for the analysis of the anions. In the case of cations, 20 mM CH_4SO_3 as mobile phase and 59 mA of suppression current at 1 $\text{mL}\cdot\text{min}^{-1}$ flow were used. In both cases the Chromaleon 6.60-SPIa software (Dionex Corporation, Thermo Scientific, USA) was used.

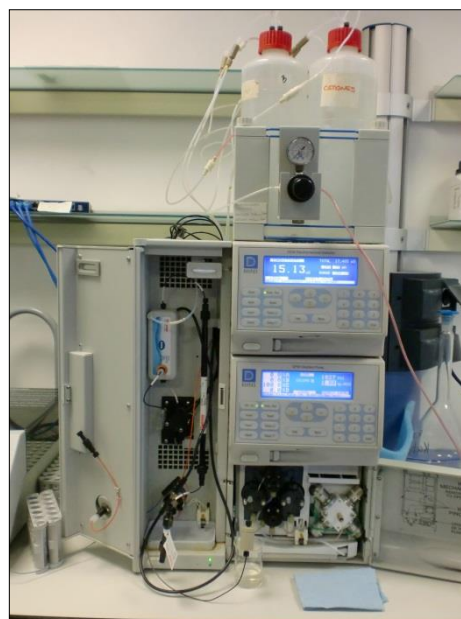


Fig 3.9. Dionex ICS 2500 ionic chromatograph

3.2.7. Inductively Coupled Plasma – Mass Spectrometry (ICP-MS)

This technique was employed for fulfilling two different objectives. On the one hand, the water where the samples were immersed was analysed in order to see the trend of the leached metals with time. These analyses were carried out taking 1 mL of that water every hour during 48 hours. The time of this experiment was set taking into account the results obtained in the potentiometric measurements since it was seen that 48 h was the time needed to reach potential stability in the system. On the other hand, the extracts measured by IC were also measured by ICP-MS, in order to determine and quantified the metals related to the soluble salts. For that purpose, an ICP-MS NexION 300 (Perkin Elmer, Ontario, Canada, Fig 3.10) inside a clean room (class 100), was used. Argon (99,999%, Praxair, Spain) was used as carrier gas. The established parameters were: nebulized flow $0.9\text{-}1\text{L}\cdot\text{min}^{-1}$, plasma flow $18\text{L}\cdot\text{min}^{-1}$ and power RF 1500W. All the samples were acidified with 1% of HNO_3 (65%) and all plastic material in contact with samples was soaked in 10% HNO_3 bath at least 24 h and finally rinsed with deionized water before use.



Fig 3.10. ICP-MS NexIon 300 (Perkin Elmer)

3.2.8. Chemical and thermodynamic modelling

In order to predict the formation of some compounds present in the steel surface, thermodynamic models were checked using information of stability constants included in the free academic software HYDRA (Hydrochemical Equilibrium-Constant) and Medusa 32 bit version (Make Equilibrium Diagrams Using Sophisticated Algorithms)³⁷ from the Royal Institute of Technology of Stockholm, Sweden. MEDUSA is based on solgaswater algorithm³⁸ and HALTAFALL algorithm³⁹.

4. RESULTS AND DISCUSSION

In this section, the results obtained by the different techniques described previously, are exposed. In order to identify the problems of the CorTen steel structures exhibited in polluted areas or marine environments, a corrosion simulation with acid rain was made as it was described in Experimental Procedure section. The samples immersed in synthesised acid rainwater were analysed by potentiometry, ICP-MS, EDXRF and Raman and infrared spectroscopies.

By means of potentiometry, the formation of the rust layer in terms of redox potential can be explained. As it can be seen in the Figure 4.1, where the potential (mV) versus time (hours) is represented, the potential reach a stable value after 50 hours. However, before reaching that stability there are some oscillations in the potential value.

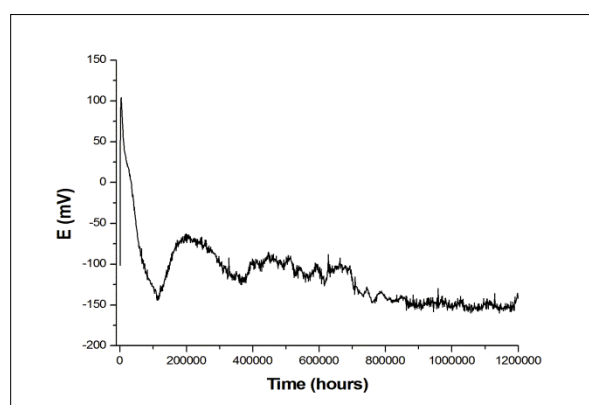


Fig 4.1. Trend of the redox potential of the solution where the samples were immersed

At the beginning, the potential is reduced due to the O_2 consumption for the formation of $FeOOH$ (Introduction, Reaction 2). Then, there is an increase of the potential due to the partial reduction of $FeOOH$ to magnetite (Introduction, Reaction 3). Finally, there is another reduction in the redox potential due to the consumption of O_2 in Reaction 4 (Introduction). It is worthy to point out that these changes in the potential are repeated until reaching de stable value. This result leads to think that the formation of the rust layer is a cyclic process, which takes place through the repetition of the described reactions several times ¹³.

In addition, this experiment was helpful to design the ICP-MS analyses of the water where the pieces were immersed because the concentration of the leached metals should reach stable value in the same time that potential did. Therefore, the water where the piece was immersed was collected each hour until 48 h since at that time the redox stability was reached.

The metal quantification experiment was performed in order to see the trend in the metal leaching. The results obtained by means of this technique are represented in the diagrams below (Fig 4.2 and 4.3) where the accumulated concentration (ng/g) versus time (hours) is represented. In the figures, it can be seen that iron is the metal which is leaching in higher concentration comparing with other metals of the steel alloy, as it could be expected. However, together with iron, it was found that manganese was also leached in high rate.

In the case of the Fe and Mn (Fig 4.2), it can be observed that the concentrations reach a stable value after 50 h, as redox potential did. This stability is achieved due to two possible reasons, either because the solution where the pieces were immersed is saturated, or because the protective rust layer is stabilised. However, other metals like nickel and copper (Fig 4.3) do not reach the mentioned stability. This is due to the fact that, these are the so called sacrifice metals, which means that they are added to the steel composition and do not reach the stability, for other metals, like in this case iron and manganese, to achieve it.

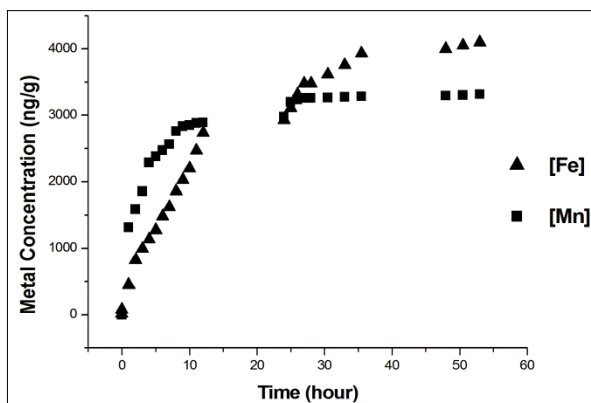


Fig 4.2. Accumulated concentration obtained by ICP-MS of leached Fe and Mn vs time

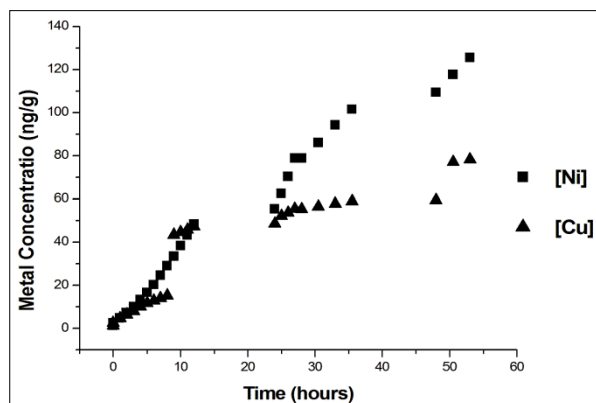


Fig 4.3. Accumulated concentration obtained by ICP-MS of leached Ni and Cu vs time

With these results and knowing the area ($\sim 5 \text{ cm}^2$) of these samples, the amount of leached metal per square metre could be calculated. The uncertainties are given in relative standard deviation form (Table 4.1). Although the observed concentration seem to be low, they can give an idea of what could be the concentration of leached metals in bigger structures such as big sculptures, facades, etc. Moreover, it must be taken into account that the quantities reflected in the table are those corresponding to 48 hours. Therefore, if the stability is not reached, metals could be leached for years, dumping high quantities of heavy metals which could have negative environmental consequences.

In contrast, some metals like chromium, are added in high amount in the initial composition of the studied steel but its quantity in the analysed water is not significant, consequently, they are not forming soluble salts in the same way than iron and manganese do (as it will be seen later).

Table 4.1. Amount of leached metal (mg) per sample area (m²) in 48 h

Metal	Fe	Mn	Ni	Cu	Cr
Quantity (mg/m²)	1,78±0,05	1,44±0,03	0,054±0,002	0,034±0,001	0,0022±0,0001

Regarding the elemental composition of the alloy, it was provided by the steelwork, however, the technique used for the characterization and its related uncertainty was unknown. Therefore, in order to provide more information about elemental composition of the steel, EDXRF analyses were carried out after the ageing tests. First of all, a reference material was measured to determine what the most appropriate method, provided by the fabricant, for the sample analyses was. Reference material data and composition given by the handheld device are summarized in Table 4.2. The uncertainties associated to the concentrations are given in standard deviation form.

Table 4.2. Elemental composition (%) of a reference material analysed by EDXRF using ALLOW LE method.

Metal	Fe	Mn	Ni	Cu	Cr	
Reference material data	---	0,82	0,44	0,22	0,58	
Data given by handheld	Concentration (%)	97,77±	0,83±	0,467±	0,21±	0,567±
		0,04	0,04	0,006	0,00	0,006

In order to see if there were differences between the reference material data and the composition obtained by EDXRF device, paired t-tests were performed. Student's t-test confirmed, at 95% of confidence level, that there were not significant differences between the results, so, Alloy LE method was selected for the sample analysis since other methods provided worse results.

EDXRF results revealed that the samples analysed were composed by iron, chromium, nickel, copper and manganese. All elemental values obtained from the media of 5 replicas (%) with their uncertainties (SD) are summarized in Table 4.3. In this case, it is

showed only the results of one sample, but the same experiment was carried out with all the samples.

Table 4.3. Elemental composition (%) of a sample immersed in rainwater analysed by EDXRF

Metal	Fe	Mn	Ni	Cu	Cr
Sample immersed	98,962±	0,074±	0,264±	0,0120±	0,0300±
	0,051	0,011	0,017	0,0045	0,071

Regarding the results obtained for the different samples, at the beginning it was supposed that all results were going to be comparable since the depth reached by the X-Ray given by the hand-held device was the same in all the analyses performed in the different samples, considering that they are made in the same material and the protective rust layer should be more or less the same. Nevertheless, after a student's test-t study, it could be affirmed that, at 95% of confidence level, there were significant differences between the results obtained for different samples in some of the detected metals, such as Ni, Cu and Cr. When the experiment were designed, it was pretended that the conditions in all the experiments were the same, however, taking into account the showed results, it could be assured that a little change in the conditions (at first sight, inestimable) could cause a significant change in the composition of the outer part of the steel.

By means of Raman and IR spectroscopies, molecular information of the composition on the protective layer was obtained. According to these results, it can be said that the main mineral phases present in the rust layer were lepidocrocite and goethite. Moreover, another iron oxide, hematite ($\alpha\text{-Fe}_2\text{O}_3$), was found. All these phases were detected by Raman spectroscopy (Fig 4.4).

Lepidocrocite is the first step in the layer formation and, actually, it was detected in most of the spectra through its Raman bands at 248 (s), 303 (w), 375 (s), 523 (m) and 645 (w) cm^{-1} . Goethite arises from the transformation of lepidocrocite with the exposure time. In this way, it was difficult to find it in the studied samples because its formation requires more time. However, in some cases it was identified thanks to its main bands at 301(m), 386 (s) and 545 (w) cm^{-1} together with $\gamma\text{-FeOOH}$, never as a pure compound. Regarding hematite, which was detected thanks to Raman bands at 224 (s), 290 (vs),

408 (s), 494 (w) and 608 (m) cm^{-1} , is not very common compound in the protective layer but it is usually developed in SO_2 rich environments ³.

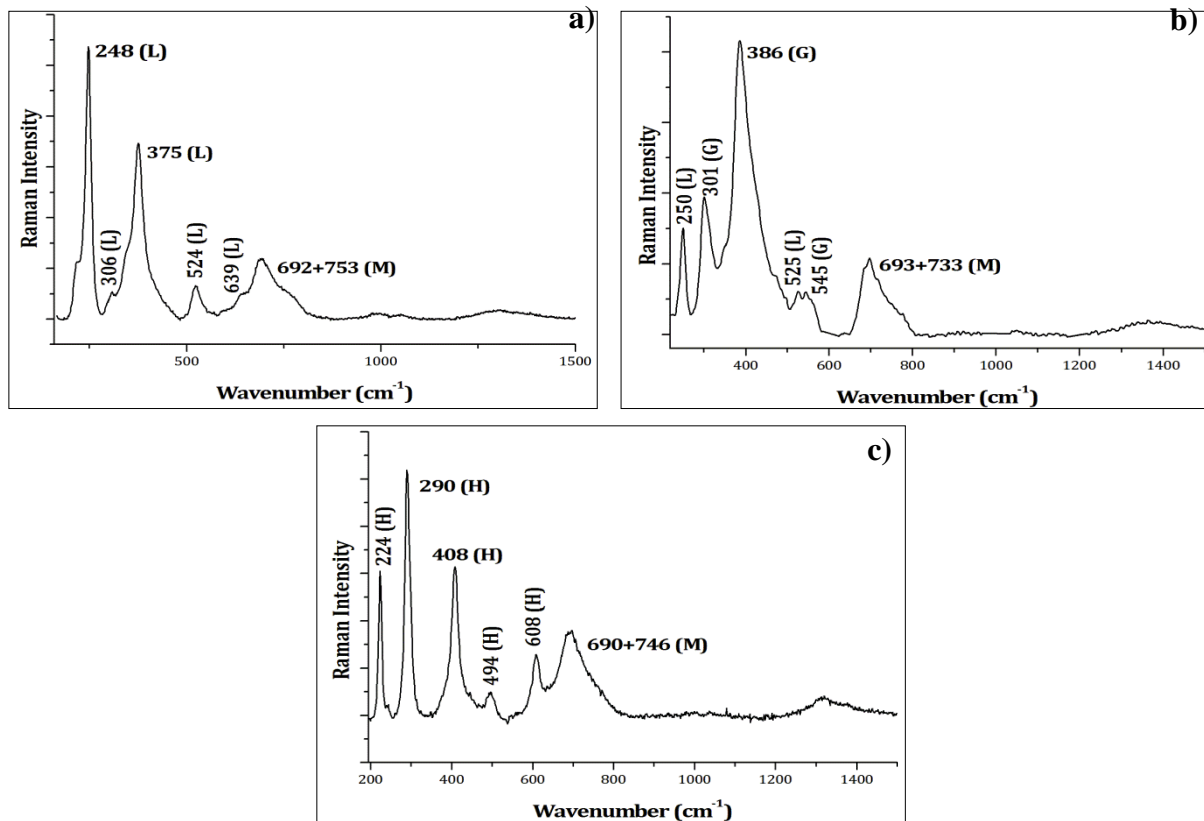


Fig 4.4. Raman spectra of immersed samples. a) Lepidocrocite (L) and maghemite (M); b) Goethite (G), lepidocrocite (L) and maghemite (M); c) Hematite (H) and maghemite (M)

As it can be seen in the previous Raman spectra (Fig 4.4), some broad bands appeared commonly in the obtained spectra due to overlapping of various Raman signals in the same spectrum range. This phenomenon was seen in most of the spectra and, for that reason, Gaussian and Lorentzian decomposition was performed in order to identify the different Raman signals that were contributing in that area. In Figure 4.5, a decomposition with bands corresponding to maghemite ($\gamma\text{-Fe}_2\text{O}_3$), which is an amorphous compound that arises of the heating of lepidocrocite, is showed ²⁶. Moreover, ferrihydrite ($\text{Fe}_2\text{O}_3 \cdot 3\text{H}_2\text{O}$), which is a low crystallinity phase composed of different types of disordered materials ²⁹, was also identified. The presence of amorphous phases was expected since the analyses were carried out in the first stages of the protective rust layer formation.

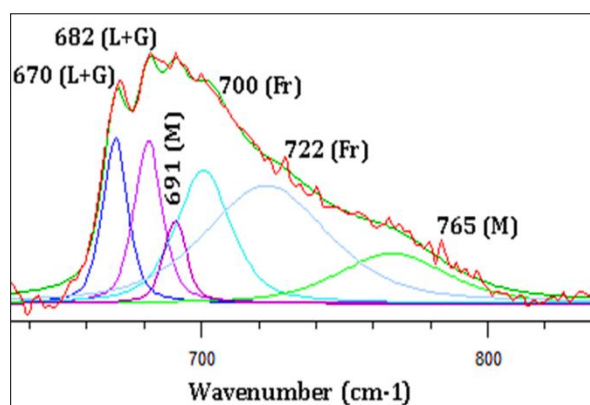


Fig 4.5. Decomposition of a broad band where amorphous phases such as maghemite (M) and ferrihydrite (Fr) together with lepidocrocite and goethite (L+G) can be seen

Moreover by Raman spectroscopy, apart from those iron phases, a manganese oxide with its main band at 580 cm^{-1} could be found (Fig 4.6).

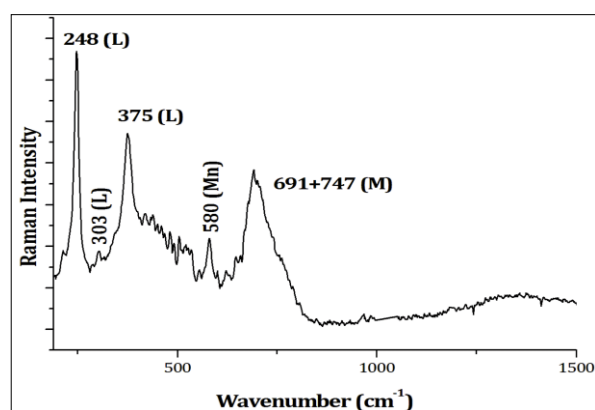


Fig 4.6. Raman spectrum of lepidocrocite (L) and maghemite together with main band of manganese oxide (Mn)

Some of these results can be supported by IR spectroscopy. All IR spectra show an important absorption in the range from 3000 to 3600 cm^{-1} characteristic of the O-H stretching band of water. Besides, bands at ~ 2330 and $\sim 2363\text{ cm}^{-1}$ corresponding to the vibrations of atmospheric CO_2 can be observed. In addition, some bands of iron phases identified also by Raman spectroscopy were detected by IR (Fig 4.10). Lepidocrocite with IR bands at 74 and 1023 cm^{-1} , goethite thanks to its band at 890 cm^{-1} and hematite with a band at 451 cm^{-1} were found. On the other hand, akaganeite with its main band at 419 cm^{-1} and feroxyhyte ($\delta\text{-FeOOH}$) with its IR bands at 484 and 1122 cm^{-1} were also detected. The first one could be detected by Raman as it is described above; and the second one has only weak broad band which are hard to detect because they are overlapped with lepidocrocite and goethite main bands^{40, 41}. Therefore, in addition to

confirm the information obtained by Raman, it could be affirmed the presence of another amorphous phase, the feroxyhyte.

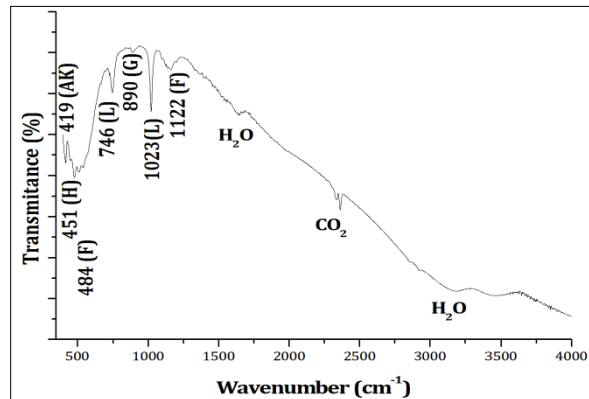


Fig 4.10. IR spectrum of immersed samples. Lepidocrocite (L), goethite (G), hematite (H), feroxyhyte (F) and akaganeite (AK)

In the case of soluble salts formed on the steel surface, by means of Raman spectroscopy, some bands located on the spectral range at 980-990 (Fig 4.7. a)) and 1020 and 1104 cm^{-1} (Fig 4.7. b)) could be recorded. These bands are in consistence with the presence of sulfates ⁴². Due to its low intensity and to the impossibility of determining the secondary bands, the presence of sulfates could be affirmed but it could not be accurately identified. However, it can be said that the most likely sulfates detected by Raman spectroscopy are those of iron and/or manganese since their sulfates Raman bands appear in this region, their oxides were also found, and, moreover, they are the most lixiviated metals according to ICP-MS results.

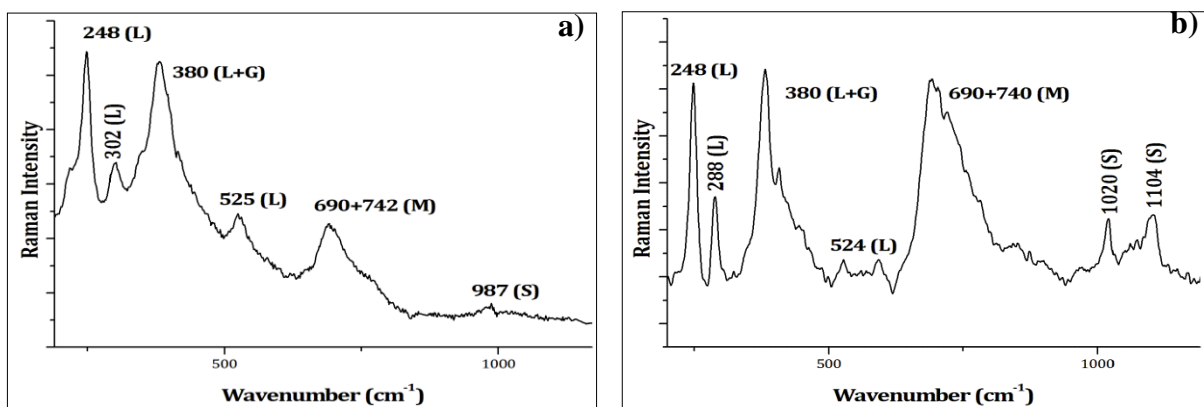


Fig 4.7. Raman spectra with the band of sulfates identified (S), together with lepidocrocite (L), goethite (G) and maghemite (M)

In order to know more about the sulfate formation on the steel surface and to check the previously stated hypothesis, thermodynamic models were performed. According to the model (Fig 4.8), in the conditions in which the experiments were carried out (pH 5,3), iron, manganese and nickel sulfate are formed ¹³ which is in concordance with what the

ICP-MS results revealed. In addition, the model estimated the fraction of the different sulphates formed and they were once again in concordance with the leaching tests, iron is the most lixiviated one because its sulphate is the predominant one, followed by manganese and finally, nickel.

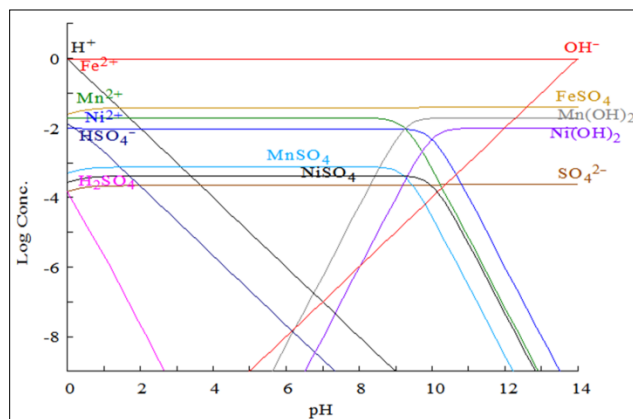


Fig 4.8. Thermodynamic model of iron, manganese and nickel sulfates formation.

Finally, also by Raman spectroscopy, bands corresponding to akaganeite (Fig 4.9) were found. This compound, as it was said in the Introduction section, is formed in presence of chloride which, in this case, comes from the salts that compound the rainwater (NaCl, KCl and $\text{CaCl}_2 \cdot 2\text{H}_2\text{O}$). Besides, it can be seen a band at 980 cm^{-1} corresponding, as it has mentioned above, to sulfates.

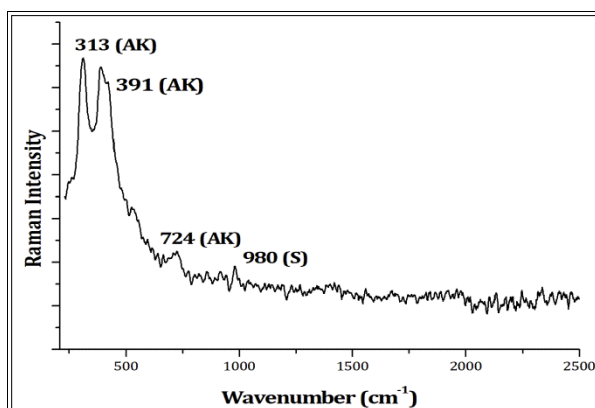


Fig 4.9. Raman spectrum of akaganeite (AK) of immersed samples and a band corresponding to sulfates (S)

On the other hand, the marble slab (Experimental Procedure, Fig 3.3) where one piece of CorTen steel was placed, was analysed by means of EDXRF with the aim of support the results obtained by ICP-MS and to see the behaviour of a porous material in contact with leached metals. With the results obtained, it could be confirmed again that iron and manganese were deposited on the surface in high extent, followed by nickel (Table 4.4). This fact means that, after the leaching of the metals, probably in soluble salt form, they

precipitate again in oxide form, which is the stain that it can be seen in the Figure 3.3. Moreover, as it is shown in Table 4.4, the concentration of leached metal, with its uncertainty indicated in total standard deviation, decreased with the distance from the sample. Knowing and taking into account that marble is a porous material, this experiment can be compared with a real situation in which a sculpture or a facade is in contact with a ground made of porous material, causing stains in the ground which are very difficult to eliminate.

Table 4.4. Metal concentration in the marble slab stain (% wt)

Metal	Fe	Mn	Ni	Cu
Blank	<LOD	72±20	33±5	<LOD
Point 1 (0 cm)	97712±183	851±28	256±9	31±5
Point 2 (2 cm)	3920±37	79±14	<LOD	<LOD
Point 3 (4 cm)	2928±36	72±17	21±4	<LOD
Point 4 (6 cm)	2600±33	95±17	20±4	16±3
Point 5 (8 cm)	2307±30	50±15	21±4	<LOD

On the other hand, in order to see the results obtained in a real situation, the sample exposed to the weather was also analysed by means of Raman spectroscopy to characterize the rust layer. Besides, for the quantification of soluble salts, IC and ICP-MS analyses were carried out. In this case, the exposure time was higher than in the previous case, so there were more reactions with acid gases (come from the atmosphere), chlorides (due to the marine airborne) and other stressors. Therefore it should be easier to find the compounds that are causing the damage.

By Raman spectroscopy, as in the other samples, even if the exposure time was longer, the main component found was lepidocrocite (Fig 4.11. a)). This rust layer phase could appear due to the fact that goethite needs more time for forming (around decades ³) and/or because analyses were performed in the surface of the rust layer where normally lepidocrocite is the main phase because it is the iron compound that appears due to the contact with atmosphere ⁴³. In addition, hematite was also found (Fig 4.11. b)), which lead to think that SO₂ has affect the evolution of the rust layer ³.

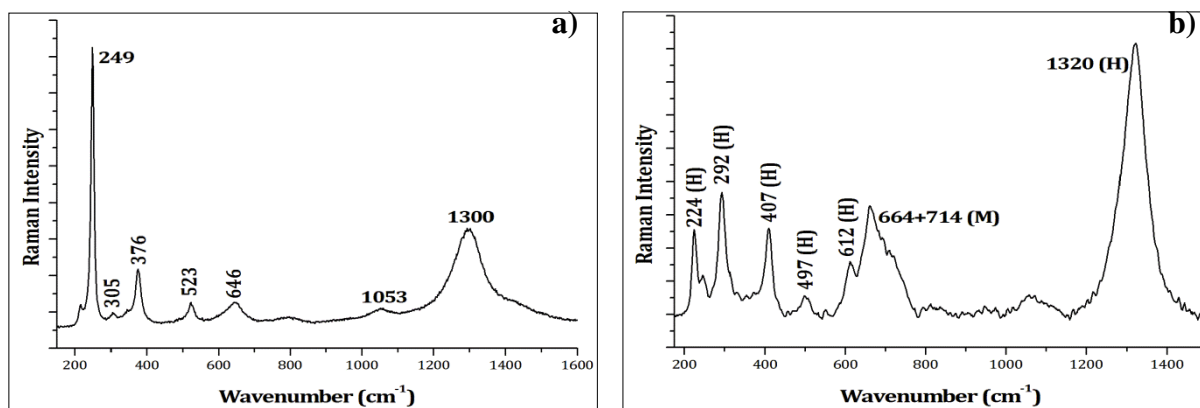


Fig 4.11. Raman spectra of the sample exposed to the weather. a) Lepidocrocite; b) Hematite (H) and maghemite (M)

Besides, regarding degradation compounds, due to the location of the sample akaganeite (Fig 4.12) and sulfates were detected. In this case, it was possible to identify the sulfate through its main Raman band at 1021 cm^{-1} (as in the same way of Fig 4.7. b)) and one of its secondary bands at 1094 cm^{-1} which correspond to an iron sulfate, lausénite ($\text{Fe}_2(\text{SO}_4)_3 \cdot 6\text{H}_2\text{O}$).

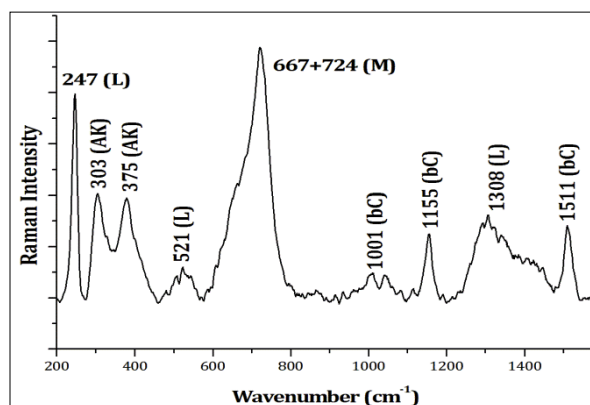


Fig 4.12. Raman spectrum of akaganeite (AK), lepidocrocite (L), maghemite (M) and beta-carotenoids (bC) collected on the exposed sample.

Apart from the iron phases which were expected, calcite (CaCO_3) and carotenoids were found (Fig 4.12 and 4.13). Calcite comes from the deposition of atmospheric dust, being one of the most abundant particulate matters in the Basque Country because of its calcareous lands ⁴⁴. On the other hand, carotenoids, concretely β -carotenoids, are biomarkers for lichen and moss presence since they occur in the pigmentation of these organisms (Fig 4.14). Besides, they are excreted by microorganisms as a mechanism to increase their resistance to extreme environments, like those with high concentration of acid gases ⁴⁵. The climatic parameters such as temperature, solar radiation and humidity, are decisive in the growth of microorganisms with biodeteriorative capability ^{46, 47}. Due to the fact that the sample was exposed to different environmental conditions

(characteristic of the climate), these molecules has grown in the entire sample surface being observed in most of the spectra.

Once the presence of soluble salts in the steel surface was detected and knowing that

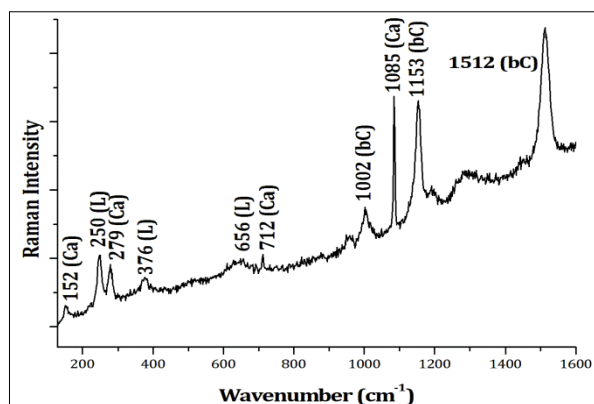


Fig 4.13. Raman spectrum of calcite (Ca), β -carotenoids (bC) and some bands of lepidocrocite (L)

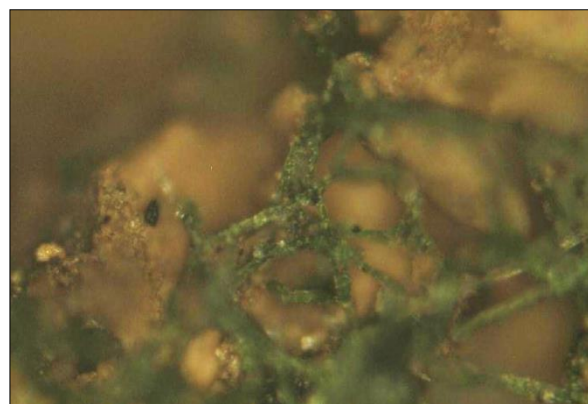


Fig 4.14. Microphotograph of the steel surface with a microorganism

they can damage the material and that they could cause an important environmental impact, a solution to remove these compounds was proposed. Ion exchange resin was selected for that purpose, as it has been mentioned before.

The results of the experiments performed by means of IC and ICP-MS are summarized in Table 4.5. The anions and cations uncertainties are given in relative standard deviation. The limit of quantification (LOQ) was calculated following IUPAC rules, defined as blank signal plus 10 SD, where SD is the standard deviation of 4 measurements of a blank.

As it was expected, taking into account that the resin is anionic, sulfate, nitrate and chloride concentrations decreased in the steel surface after the treatment. Based on the obtained results, it can be affirmed that the proposed solution is valid, and the compounds that cause the damage on the steel structures were removed. However, as the table shows, most of the cations and metals decreased too. Due to the fact that the system has to maintain the electro neutrality, cations have to decrease in the same way that the anions do. Therefore, it is thought that these compounds are being leached with the water used to compact the resin, which could cause a major environmental impact. However, it had to be taken into account that, this damage was not representative because, this leaching would have happened likewise, with the rainwater, so the environmental impact would not be increased by the resin treatment. In Figure 4.15 it can be seen the loss percentage of each ion.

CorTen Steel: a solution to atmospheric degradation in acid and marine environments

Table 4.5. Soluble salts concentrations determined by ion chromatography and ICP-MS in mg·kg⁻¹. PRE-RESIN TREATMENT / POST-RESIN TREATMENT

[Na ⁺]	[NH ₄ ⁺]	[K ⁺]	[Ca ²⁺]	[Cl ⁻]	[NO ₃ ⁻]	[SO ₄ ²⁻]	Fe	Mn	Ni	Cu	Cr
1,75±	0,485±	1,82±	6,36±	2,38±	<LOQ	3,83±	0,193±	0,0036±	0,0039±	0,0030±	0,0030±
0,36	0,003	0,32	0,36	0,49	<LOQ	0,33	0,009	0,0002	0,0002	0,0002	0,0001
0,428±	0,573±	0,46±	5,15±	1,33±	<LOQ	1,89±	0,030±	0,00055±	0,0016±	0,0032±	0,0023±
0,088	0,010	0,26	1,23	0,42	<LOQ	1,17	0,002	0,00004	0,0001	0,0002	0,0001

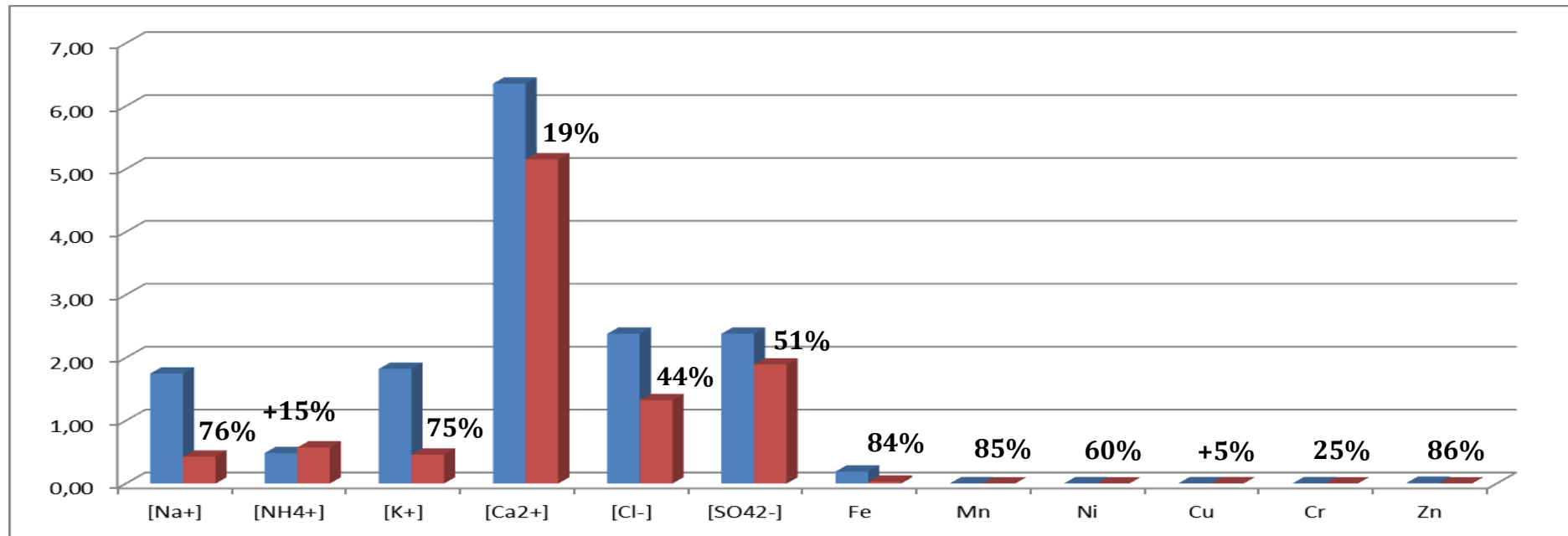


Fig 4.15. Loss percentage of each ion. Some of them increase as in the case of ammonium and copper.

5. CONCLUSIONS

Following the analyses performed by different methods the composition of protective layer was determined and which metals were being leached and what was their trend was quantified.

The potential changes could be related with the wet/dry cycles, corresponding to each change with one reaction involved in the layer formation. On the other hand, ICP-MS analyses showed which metals were leaching, in which amount and what the followed trend was. Based on the results, it could be affirmed that iron, manganese and nickel were the metals which were leached in higher amount, a fact confirmed by the EDXRF analyses carried out over the marble slab, obtaining the same leached metals with both techniques. The leached metals have their own function in the steel. For example, manganese and nickel are added in order to increase hardenability and to decrease weldability. Consequently, leaching of these metals can involve a loss of those properties, reducing the quality of the material and, therefore, causing detachments or discolorations in the surfaces as it has seen in Introduction section. This fact is very important when using this material for artworks, since in a short period of time the work could be very different from the one designed by the artist.

The results obtained by EDXRF on the samples, showed, thanks to the *Student's t-tests*, that a little change in the environmental conditions could lead in big differences in the composition of the surface of the steel. With these results, the importance of the location where a weathering steel structure is exposed could be observed, because, it could involve, not only structural damages as it has seen before, but also an environmental impact due to the formation of soluble salts of metals which compound the steel. Besides, with the scaled concentrations obtained with ICP-MS and EDXRF, and related to the dimensions of the analysed pieces of steel, it could be confirmed that the amount of metals leached can be important and it should be taken into account, to know the environmental effects that larger structures could cause due to the toxicity of these elements in high concentration. These leached metals can affect the soil, the groundwater

reaching rivers and sea, and finally they could be introduced in the food chain producing many diseases.

Furthermore, as it can be seen in all analysed samples and as it was expected, the major components in the rust layer were lepidocrocite, goethite and hematite. It could be affirmed that lepidocrocite is formed in the first stages of atmospheric corrosion, and due to the short time of exposure (2 weeks), is the most found compound. In addition to these common phases, it was also identified some amorphous compounds such as, maghemite and ferrhydrite, showing that even if accelerated essays were carried out, the protective layer was still not passivated and therefore, it was not exerting any protective function. The IR analyses done with the samples immersed in rainwater were useful to support the Raman results being possible to identify the same mineral phases and, moreover, it was possible to observe another amorphous phase, feroxyhyte, which is very difficult to detect by Raman spectroscopy because it is very amorphous phase and it is difficult to distinguish from other compounds with broad bands.

Apart from the exposure time, the influence of the environment in where the samples are exhibit can be seen evaluated based on the data extracted from this work. In this case, the contact with inorganic salts such as sulphates and chlorides, leads to the formation of the metal sulphates and akaganeite which were detected by Raman and IR spectroscopies and damage steel structure. It have to be taken into account that in most of the cases, the problem found was related with metal sulphates, so it could be affirmed that the most harmful compound was de SO_2 .

Taking into account that soluble salts, sulphate among all, were the responsible for the observed problems, the anionic resin treatment seemed to be the better option for the consolidation of this material when it is exposed to acid and coastal environments. With the obtained results, it could be affirmed that anions which were increasing the corrosion rate of the steel and, at the end, causing the material loss problem, were removed by the resin and consequently that problem, was solved. However, it must be said, that ICP-MS results showed that the amount of metals also decreased.

Notwithstanding, this fact does not seem to be a negative aspect because the leaching of those metals would have occurred anyway by the effect of the rain. Actually, they were removed only by the water present in the resin when it was applied. Therefore, the only presence of moisture, for instance, would have removed them in a real situation since they are forming very soluble salts. To sum up, the resin treatment resulted very suitable to remove sulphates and chlorides which have been proved to be the most aggressive agents against the normal development of the weathering steel.

6. BIBLIOGRAPHY

1. Weng Y., Dong H., Gan Y., *Advanced Steels. The recent scenario in steel science and technology*. Metallurgical Industry Press. **2011**, Beijing.
2. Nayar A. *The steel handbook*. Tata Mc.Graw Hill. **2000**, India.
3. Aramendia J. Ph. D. Thesis. UPV-EHU, Basque Country, Spain, **2013**.
4. Davis J. R., *Alloying: Understanding the basics*. ASM International. **2001**, Ohio.
5. Kumar Saha J., *Corrosion of constructional steels in marine and industrial enviroment*. Engineering Materials. **2013**, India.
6. Aramendia J., Gómez-Nubla L., Bellot-Gurlet L., Castro K., Paris C., Colomban P., Madariaga J. M. J. Raman Spectrosc. **2014**, 45, 1076.
7. Frankel G. S., Isaacs H. S., Scully J. R., Sinclair J. D., *Corrosion Science: A retrospective and Current Status in Honor of Robert P. Frankenthal*. The Electrochemical Society. **2002**, New Jersey.
8. Damgaard N. R., Ph. D. Thesis. University of Waterloo, Ontario, **2009**.
9. Huang H., Zhu Y. Corros Sci. **2005**, 47, 1545.
10. Misawa, T., Asami, K., Hashimoto, K., Shimodaira, S.: Corros. Sci. **1974**, 14, 279.
11. Aramendia J., Gómez-Nubla L., Arrizabalaga I., Prieto-Taboada N., Castro K., Madariaga J. M. Corros Sci. **2013**, 76, 154.
12. Morcillo M., Díaz I., Chico B., Cano H., de la Fuente D. Corros Sci. **2014**, 83, 6.
13. Ruiz P., Aramendia J., Carrero J. A., Castro K., Madariaga J. M., Arana G. Applied Phisics A. **2016**, Under review.
14. Arroyabe C., Morcillo M. Corros. Sci. **1995**, 37, 293.
15. Oesch S. Corros Sci. **1996**, 38, 1357.
16. Hao L., Zhang S., Dong J., Ke W. Corros Sci. **2012**, 58, 175.
17. Nomura K., Tasaka M., Ujihira Y. Corrosion. **1988**, 44, 131.
18. Millar G. J., Couperthwaite S. J., Papworth S. Journal of Water Process Engineering. **2016**, 11, 60.

-
19. Zaganianis E. J., *Ion exchange resins and synthetic adsorbents in food processing*. **2009**, Paris, France.
 20. Wachinski A. M., Etzel J. E., *Environmental ion exchange. Principles and design*. CRC Lewis Publishers. **1997**, New York.
 21. Wheaton R. M., Lefevre L., J. DOWEX Ion exchange resins. Fundamentals of ion exchange. The Dow chemical company. **2000**.
 22. Quevauviller Ph., Ebdon L., Harrison R. M., Wanh Y. *The Analyst*. **1998**, 123, 971.
 23. Cazallas López R. Ph. D. Thesis, UPV-EHU, Basque Country, Spain. **1997**.
 24. Castro K., Pérez-Alonso M., Rodríguez-Laso M. D., Fernández L. A., Madariaga J. M. *Anal. Bioanal. Chem.* **2005**, 382, 284.
 25. Froment F., Tournié A., Colomban Ph. *J. Raman Spectrosc.* **2008**, 39, 560.
 26. Hanesch M. *Geophys. J. Int.* **2009**, 177, 941.
 27. Prieto-Taboada N., Ibarrodo I., Gómez-Laserna O., Martínez-Arkarazo I., Olazabal M. A., Madariaga J. M. *J. Hazardous Materials*. **2013**, 248-249, 451.
 28. De Gelder J., De Gussem K., Vandenabeele P., Moens L. *J. Raman Spectrosc.* **2007**, 38, 1133.
 29. Cano H., Neff D., Morcillo M., Dillmann P., Díaz I., de la Fuente D. *Corros Sci.* **2014**, 87, 438.
 30. Jaén J. A., Garibaldi G. *Tecnociencia*. **2004**, 6, 137.
 31. Murad E., Bishop J.L. *American Mineralogist*. **2000**, 85, 716.
 32. Parameshwari R., Priyadarshini P., Chandrasekaran G. *American Journal of Materials Science*. **2011**, 1, 18.
 33. Purolite ® A-100. Weak base anion macroporous resin. Product data sheet. Purolite.
 34. Guimarães D., Leão V. A. *Journal of Environmental Management*. **2014**. 145, 106.
 35. Martínez Arkarazo I. Ph. D. Thesis, UPV-EHU, Basque Country, Spain. **2007**.
 36. Field methods for retrieval and analysis of soluble salts on steel and other nonporous substrates, SSPC Technology guide 15. Pittsburg, **2005**.

37. Puigdomenech, I. MEDUSA (Make Equilibrium Diagrams Using Sophisticated Algorithms), version 15; Department of Inorganic Chemistry, The royal Institute of Technology: Stockholm, Sweden. <http://www.kth.se/che/medusa>
38. Eriksson G. *Anal.Chim.Acta.* **1979**, 112, 375.
39. Ingri N., Kakalowicz W., Sillén L. G., Warnqvist B. *Talanta.* **1967**, 14, 1261.
40. Dunwald J., Otto A. *Corros. Sci.* **1989**, 29, 1167.
41. Guzonas D. A., Rochefort P. A., Turner C. W. *Corrosion product characterization by fibre optic raman spectroscopy.* Atomic Energy of Canada Limited. Chalk River Laboratories. Ontario, Canada.
42. Frost R., Wills R-A., Martens W. *Journal of Raman Spectroscopy.* **2005**, 36, 1106.
43. Neff D., Bellot-Gurlet L., Dillmann Ph., Reguer S., Legrand L., J. *Raman Spectrosc.* **2006**, 37, 1228.
44. Inza A. Ph. D. Thesis. UPV-EHU, Basque Country, Spain, **2010**.
45. Aramendia J., Gomez-Nubla L., Bellot-Gurlet L., Castro K., Arana G., Madariaga J. M. *International Biodeterioration & Biodegradation.* **2015**, 104, 59.
46. Edwards H. G. M., Russell N. C., Seaward M. R. D. *Spectrochim. Acta A.* **1997**, 53, 99.
47. Withnall R., Chowdhry B. Z., Silver J., Edwards H. G. M., de Oliveira L. F. C. *Spectrochim. Acta A.* **2003**, 59, 2207.

7. APPENDIX

7.1. SCIENTIFIC PUBLICATIONS

7.1.1. Articles

- Ruiz P., Aramendia J., Carrero J. A., Castro K., Madariaga J. M., Arana G. *Applied Physics A*. **2016**, Under review.

7.1.2. Congresses

International congress, Poster:

Authors: Ruiz P., Aramendia J., Castro K., Madariaga J. M.

Congress: inArt Congress 2016. 2nd International Conference on Innovation in Art Research and Technology.

Place and date: Ghent, Belgium. 21/03/2016 - 25/03/2016

Title: Effect of acid rain on the leaching of heavy metals from CorTen steel structures.

International Congress, Poster

Authors: Ruiz P., Aramendia J., Gómez-Nubla L., Castro K., Madariaga J. M.

Congress: GeoRAMAN-2016. XII International Conference.

Place and date: Novosibirsk, Russia. 09/06/2016 – 15/06/2016

Title: The degradation of Mn in CorTen steel affected by acid rain.



Gestión del paisaje. Patrimonio, territorio y ciudad
Paisaiaren kudeaketa. Ondarea, lurraldea eta hiria
Landscape management. Heritage, territory and city

Weathering steel has a special resistance against the atmospheric corrosion through the formation of a protective layer. This layer is formed, among others, due to the reaction of some alloy elements present in the steel with reactive species, such as sulphur and nitrogen oxides and/or chlorides, which are present in the environment. For that reason, it is a widely used material in outdoor structures (facades, bridges) and it is in vogue among modern sculptors because this material changes its texture and colour with the pass of time and with the environment in which is exhibited. However, depending on the location, some problems could appear in the development of the protective layer. For instance, even if the acid gases collaborate in the formation of the rust layer, when they appear in high concentration they can be counter-productive in the well development of the protective layer. In fact, acid rain and marine aerosol can accelerate the corrosion process causing the leaching of some steel alloy metals. In consequence, the corrosion can be the responsible of the destruction of the structure, and moreover, the responsible of several negative environmental impacts due to the toxicity of those leached metals. In this work spectroscopic techniques were used in order to determine the composition of protective layer, both the original composition and the degradation compounds formed due to the reaction of the material with the surrounding atmosphere. On the other hand, quantitative techniques, as well as monitoring the quantity of leached metals, they were helped in the development of a solution for the damage caused by chlorides and acid gases, being sulphates the most worrying stressors. For that purpose a ion exchange resin was employed with the aim of removing sulphates, chlorides and nitrates, and thus, avoiding the destruction of the steel structure.

Resumen/Laburpena/Summary

eman ta zabal zazu



Universidad del País Vasco Euskal Herriko Unibertsitatea